Microscopic model for the formation of nanodomains in relaxor materials

Manuel I. Marqués[*] and Carmen Aragó

Departamento de Física de Materiales C-IV, Universidad Autónoma de Madrid, 28049 Madrid, Spain

A microscopic relaxor model is presented and its properties are studied by means of numerical simulations. No "*a priori*" random interactions or random fields are considered. The sole interaction of mobile charges with the dipoles of a highly polarizable medium is responsible for the appearance of typical relaxor properties such as a smeared transition, a glassy ground state with no macroscopic polarization, an external field frequency-dependent dielectric constant, and a field-induced ferroelectric behavior. The model shows no statistical difference between the relaxor and the ferroelectric formation of polar nanoregions at high temperature. However, for the relaxor, there is a temperature (which we associate with the Burns temperature) below which some dipoles, neighbors to the charges, get frozen with a net square polarization different from zero. These dipoles are the precursors of stable boundaries from which ferroelectric clusters grow when approaching the glassy phase. These frozen dipoles are responsible for the frequency dispersion of the dielectric constant and for the smearing of the transition.

I. INTRODUCTION

Relaxor materials are a special class of ferroelectric crystals with an intrinsic disordered structure. In recent years, the field of research devoted to the study of relaxors has experienced a revival of interest owing to their extraordinary dielectric and piezoelectric properties.[1] Applications range from piezoelectric/electrostrictive actuators and sensors to elasto-optic and photorefractive elements. The relaxor behavior was first observed in perovskites with disorder of nonisovalent ions $Pb(Mg_{1/3}Nb_{2/3})O_3$ (PMN).[2] It has been also observed in $Pb(Sc_{1/2}Ta_{1/2})O_3$ (PST) (Ref. 3) and in nonstoichiometric solid solutions such as $Pb_{1-x}La_x(Zr_{1-y}Ti_y)_{1-x/4}O_3$ (PLZT).[4,5] Also, many homovalent solid solutions such as $Ba(Ti_{1-x}Zr_x)O_3$ (BTZ) (Refs. 6 and 7) and $Ba(Ti_{1-x}Sn_x)O_3$ (BTS) (Ref. 8) exhibit relaxor behavior. Other examples of relaxor ferroelectric are complex perovskites such as $Pb(Zn_{1/3}Nb_{2/3})O_3$ (PZN), $Pb(Mg_{1/3}Ta_{2/3})O_3$ (PMT), $Pb(Sc_{1/2}Nb_{1/2})O_3$ (PSN), solid solutions, $[(1-x)Pb(Mg_{1/3}Nb_{2/3})O_3-xPbTiO_3$ (PMN-PT) and $(1-x)Pb(Zn_{1/3}Nb_{2/3})O_3-xPbTiO_3$ (PZN-PT)] and uniaxial $Sr_xBa_{1-x}Nb_2O_6$ (SBN).

Relaxors possess several features not found in ordinary ferroelectrics: (i) the dielectric permittivity response is frequency dependent, (ii) the transition at a so-called maximum temperature T_m is diffusive, (iii) there is an absence of both spontaneous polarization and structural macroscopic symmetry breaking, and (iv) ferroelectric response is obtained after field cooling.[9] The origin of these relaxor properties seems to lie in two essential ingredients, the existence of lattice disorder and the existence of polar nanoregions (PNRs) at high temperatures above T_m. The existence of PNRs is well documented but their structure and origin are still subject of controversy.[10]

The lattice defects or the chemical substitution in some relaxors induce extra charges. When cooling from high enough temperatures, these charges may lead to the formation of small polar nanoregions below the so-called Burns temperature T_d.[11] These polar nanoregions grow as tempera-

ture decreases usually leading to an isotropic state at $T < T_m$ with randomly oriented polar domains, preventing the system from ferroelectricity or antiferroelectricity. It is not clear whether these PNRs are due to phase fluctuations particularly localized in some regions of the crystal where the phase-transition temperature is higher[12,13] or if the stability of the domain state is due to local fluctuations of the quenched microscopic field.[14] Many theoretical approaches to the nature and roles of PNRs based on random fields and random bond models have been proposed.[14–18]

II. MODEL

The objective of this paper is to propose a relaxor model as simple as possible, with no "a priori" disorder included such as random fields or random interactions, to deeply study PNRs formation in relaxor systems. The model is based solely on the following two ingredients: (i) a highly polarizable lattice and (ii) charge disorder. The simplest polarizable lattice is a two-dimensional Ising system. The Ising model has a well-defined second-order phase transition from para to ferro state at a critical temperature different from zero and no field applied. As corresponding to a second-order phase transition, spontaneous polarization and symmetry breaking appears at the critical temperature and the behavior of both, order parameter and susceptibility, is given by a well-known set of critical exponents (i.e., there is no smeared transition). Ising model corresponds to a pure system with no disorder, however, when a mixed system is considered charge disorder may show up. A well-known example is the SBN crystals where negative excess charges are produced by vacancies in the bronze-tungsten structure. These charges are mobile if the temperature is high enough. For example, in SBN:Ce, the dark conductivity increases by 2 orders of magnitude at $T = 145\ °C$ when compared to its value at room temperature.[19] Based on these ideas, we consider a two interpenetrated layer system. One of the lattices is the polarizable Ising model with coupling constant J and the other lattice is where itinerant charges move (see Fig. 1). Dipoles are fixed at (i, j)
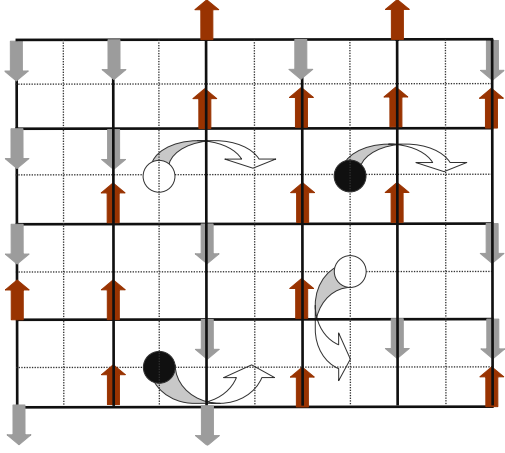
FIG. 1. (Color online) Relaxor model based on two interpenetrated lattices. Regular Ising dipoles are fixed at odd (i,j) positions (thick continuous lattice) while positive charges (white circles) and negative charges (black circles) are free to jump among empty neighboring even (i,j) positions (thin discontinuous lattice). The two different gray colors represent the two possible different dipole orientations in the Ising lattice.

lattice positions with i and j odd (in uniaxial SBN, the dipoles correspond to the ferroelectrically active Nb^{5+} ions) while charges carriers are free to jump among the different empty-lattice sites (i,j) with i and j even. To preserve charge conservation and continuity equation, charges are never created or annihilated. Also, electroneutrality is maintained during the simulations.

Nearest-neighbor dipoles interact with the usual Ising Hamiltonian,

$$H_s = -J \sum_{(i,j)\in odd} s(i,j)[s(i+2,j) + s(i,j+2)] \qquad (1)$$

with $s(i,j) = \pm 1$ depending on the dipole orientation.

Charges and nearest-neighbors dipoles interact with each other via a coupling constant J_q,

$$H_q = -J_q \sum_{(i,j)\in even} q(i,j)[s(i-1,j+1) + s(i+1,j+1)$$
$$- s(i-1,j-1) - s(i+1,j-1)] \qquad (2)$$

with $q(i,j)=1$ if the charge is positive and $q(i,j)=-1$ otherwise. If there is no charge then $q(i,j)=0$. The order-disorder and uniaxial nature of the Ising matrix proposed make this model particularly useful for SBN-like relaxors which lack of any optic soft mode[20] and can be mapped onto models with short-range interactions and negligible dipolar corrections.[21] However, for other nonuniaxial displacive relaxors, such as PMN, long-range dipolar forces should be considered. In general, dipole-dipole long-range interactions should be considered in our model for the ferroelectric (nonrelaxor) limit. These interactions are needed to obtain first-order phase-transition properties[22] and spatially modulated structures producing depolarizing fields[23] which may have important implications when considering the boundary-conditions' peculiarities of thin-layer phase transitions.[24] Also, the extension of this model to mimic more compli-
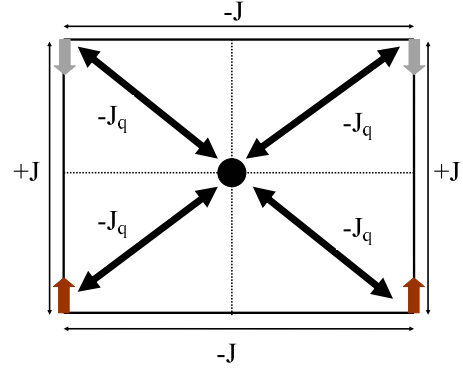

FIG. 2. (Color online) Interactions scheme for the model proposal. Next-neighbor Ising dipoles pointing into the same direction interact with a $-J$ coupling constant. If the dipoles point toward different directions then the interaction is positive $+J$. A negative charge (black circle) interacts solely with the four next-neighbor Ising dipoles. The interaction coupling is $-J_q$ if positive parts of the dipoles point toward the negative charge and $+J_q$ otherwise. For a positive charge, the situation is just the opposite (not shown). Note how itinerant charges act like domain-boundary seeds.

cated, first order, relaxor systems may be performed by considering alternative polarizable statistical models such as the Potts model.

The only physical basic idea used to propose this Hamiltonian is that negative charges attract positive parts of the dipoles while positive charges do the opposite. (see Fig. 2). Since electric fields produced by the charges are local and strongly screened,[21] no extra interaction among charges or long-range interactions between charges and dipoles are considered. The total energy on our system is given by

$$H = H_s + H_q. \qquad (3)$$

By considering this simple model, we will answer the following question: do these two simple basic ingredients (a highly polarizable lattice and charge disorder) induce a relaxor behavior? If the answer is positive then we may extract some information about the relaxor PNRs formation mechanism using this model.

The following values are used for the parameters on the simulations, $J=1/T_c$, being T_c the critical temperature of the two-dimensional Ising model obtained by Onsager,[25] $J_q=10/T_c$ corresponding to a charge-dipole exchange interaction one order of magnitude stronger than the dipole-dipole interaction. Polarization and susceptibility of the system versus temperature are calculated by extensive Monte Carlo simulations.

For each temperature, the polarization is calculated as an average of the polarization of 50 different relaxor realizations (each realization with a different initial state of dipoles and charges positions). For each realization and temperature polarization is calculated as

$$\langle P \rangle = (1/Ns) \sum_{n=1,Ns} \sum_{(i,j)\in odd} s(i,j), \qquad (4)$$

where Ns represents the total number of Monte Carlo steps (MCS) (we consider $Ns=10\,000$ and $Nt=10\,000$ steps
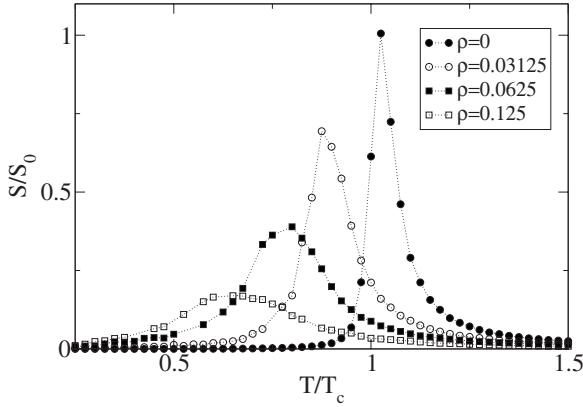
FIG. 3. Normalized susceptibility vs normalized temperature for different values of the charge-carrier density. The "transition" temperature T_m at each density value is given by the maximum of the susceptibility.
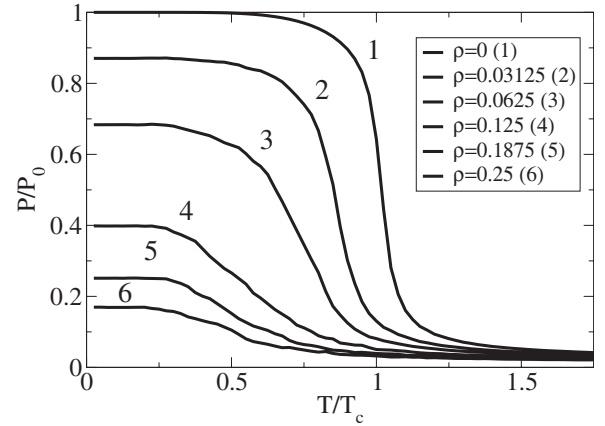

FIG. 4. Normalized polarization vs normalized temperature for different values of the charge-carrier density.

for thermalization between each temperature). All values are normalized to $P_0 = L \times L$ being $L = 80$ the lateral size of the dipole's system.

Susceptibility is calculated as thermal fluctuations of the polarization $S = (1/T)[\langle P^2 \rangle - \langle P \rangle^2]$ and frequency dependence of relaxor's susceptibility is calculated considering that only fast dipoles, compared to the frequency applied, fully contribute to the susceptibility.[26] Before average calculations are performed, the number of flips (n_{flips}) of each dipole are calculated during 500 MCS. Assigned frequency is defined as $w \equiv N_{flips}/(500 \text{ MCS})$. The maximum measuring frequency on our system is given by $w = 1$ (a flip at every attempt) and the minimum is given by the equilibrium $w = 0$ value. For a given frequency, i.e., for a N_{flips} given value, if the number of flips of a particular dipole is $n_{flips} < N_{flips}$ then the contribution to the averaged susceptibility of this dipole is weighted by n_{flip}/N_{flip}. For $w = 0$, every dipole contributes equally.

III. RELAXOR PROPERTIES

A. Smearing of the phase transition

In Fig. 3, we plot the susceptibility for different values of the charge-carrier density ρ. Charge-carrier density ρ is defined as the total number of charge carriers (positive or negative) divided by the total number of sites available ($L \times L$) or total number of dipoles. It is a dimensionless occupation ratio ranging from zero to one,

$$\rho = \frac{1}{L \times L} \sum_{(i,j) \in even} |q(i,j)|. \tag{5}$$

Note how the transition is smeared as the amount of charge disorder is increased. This behavior is very similar to the one found by Glass for relaxor $Sr_xBa_{1-x}Nb_2O_6$ (Ref. 27) where the maximum of the dielectric constant and the critical temperature decrease as randomness increases in the sample by adding Sr. ρ values smaller than one are related to relaxor samples with a smaller amount of disorder such as, for example, $(Sr,Ba,Na)Nb_2O_6$ (Ref. 28) where a decrease in the

relaxor behavior has been found when vacancies (negative excess charges) are substituted by sodium atoms.

B. Absence of spontaneous polarization and field-induced ferroelectric behavior

In Fig. 4, we plot the polarization vs temperature for different charge-carrier densities. Spontaneous polarization at $T = 0$ decreases as the amount of randomness is increased till almost no spontaneous polarization is found. As corresponding to a relaxor with remanent polarization, the slope dP/dT at T_m decreases as the amount of charge disorder is increased. The value $dP/dT \neq \infty$ at the transition for the case with $\rho = 0$ is merely due to the finite-size effects of the simulation.

It is well known that ferroelectric behavior in a relaxor may be obtained by field cooling. Actually Granzow *et al.*[19] used electric fields at high temperatures to induce a preferred direction in the relaxor SBN crystal leading to a reorientation of the domains and to a ferroelectric phase at low temperatures. They found that reorientation worked only if the temperature was applied below the so-called Burns temperature. To study if our model mimics this behavior, we polarized our system by applying a high electric field at different temperatures T_E. We consider the strong relaxor with $\rho = 0.25$. Numerical results are shown in Fig. 5, compared to the nonpolarized result. Note how, in order to obtain a change in the spontaneous polarization at $T = 0$, we must apply our fields at temperatures below $T_E/T_c \sim 3$. So we may estimate $T_d \sim 2T_c$ as the Burns temperature of the system.

C. Dielectric dispersion

In Fig. 6, we compare the dispersion of the susceptibility for a ferroelectric ($\rho = 0$) and a relaxor ($\rho = 0.125$). In agreement with experiments,[29] the relaxor exhibits a strong frequency dispersion while the ferroelectric shows no dispersion at all (see inset in Fig. 6). The relationship between the temperature of the maxima and the frequency of the electric field applied may be fitted by a Vogel-Fulcher relationship as corresponding to a relaxor glassy behavior[30] with parameters
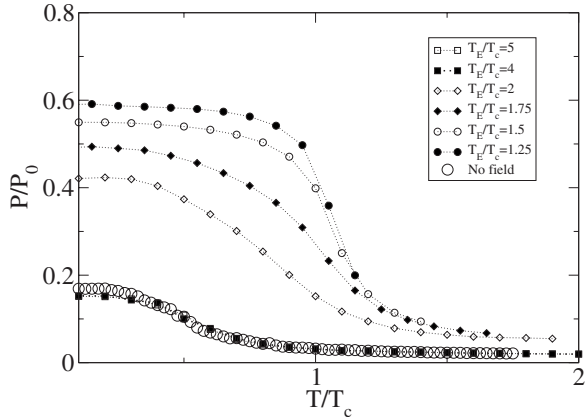
FIG. 5. Normalized polarization vs normalized temperature for a charge-carrier density value $\rho=0.25$. The electric field used to polarize the sample is applied at different polarization temperatures T_E. The polarization behavior with $T_E/T_c=4$ and $T_E/T_c=5$ coincides with the one corresponding to no field applied (white circles).

given by a static maximum temperature $T_m=0.625T_c$ and an activation energy $0.325T_c$.

D. Departure from the Curie law

In experiments, Burns temperature is sometimes obtained as the onset of departure from a linear temperature dependence of the inverse static susceptibility. We have calculated inverse static susceptibility for the ferroelectric system and for the relaxor with $\rho=0.25$. Results are shown in Fig. 7. Note how the behavior of the ferroelectric is the typical linear Curie behavior with null value at $T \sim T_c$. For the relaxor, the situation changes completely and a clear departure from the linear behavior is found for temperatures below $T/T_c \sim 3$, which is in agreement with the Burns temperature previously estimated by field-induced ferroelectric behavior calculations.

IV. NANODOMAINS FORMATION AND THE ORIGIN OF THE BURNS TEMPERATURE

Once we have checked how our Ising model with a charge-carrier density different from zero shows the most
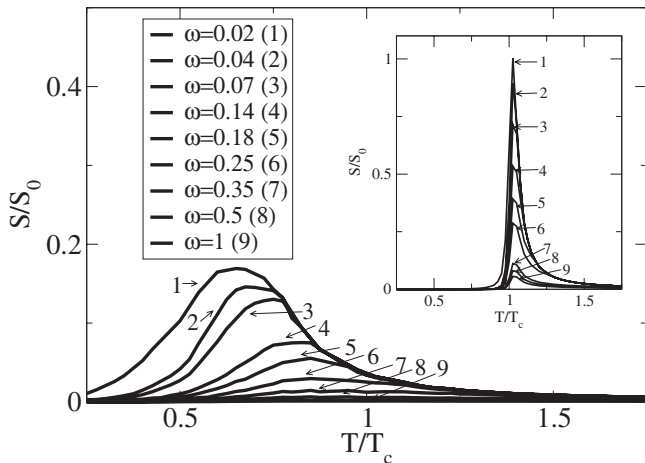

FIG. 6. Normalized susceptibility vs normalized temperature for $\rho=0.125$ and $\rho=0$ (inset) considering different ω frequencies.
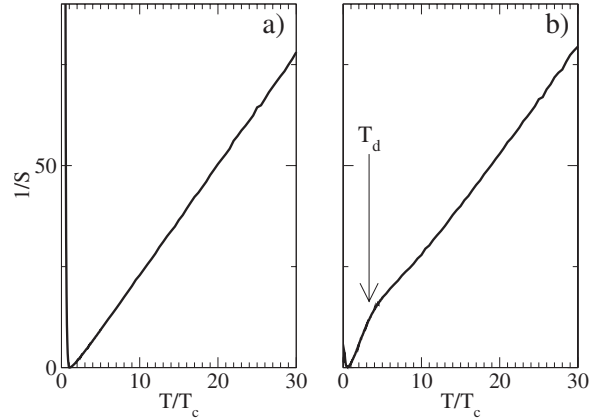

FIG. 7. Inverse static susceptibility versus normalized temperature for (a) $\rho=0$ and (b) $\rho=0.25$. Departure from a linear behavior is found for $\rho=0.25$ at temperatures close to the Burns temperature T_d. Rounding found at the critical temperature T_c is due to the interaction between individual spins in the Ising model.

important relaxor properties, we are going to study how ferroelectric nanodomains are formed and how they affect to the relaxor. Numerical calculations allow us to explicitly calculate the averaged cluster size at every temperature for $\rho=0.125$ and for the ferroelectric case ($\rho=0$). Results are shown in Fig. 8. Note how, when the system is cooled down from high temperature, almost no difference is found between the ferroelectric and the relaxor till the phase-transition critical temperature T_c is reached, then the ferroelectric monodomain is formed for the ($\rho=0$) model. The size of the clusters is very similar for both systems and no appreciable high-temperature domains formation is found for the relaxor model when compared to the ferroelectric. Actually, there is no special change on cluster size at the previously estimated Burns temperature $T_d \sim 2T_c$. We have ana-
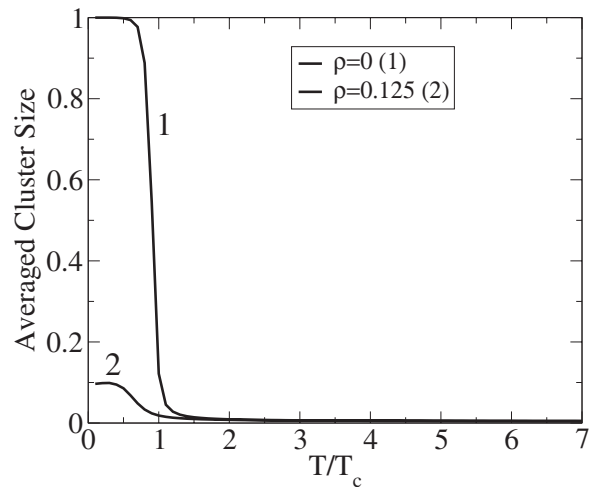

FIG. 8. Averaged cluster size vs normalized temperature for $\rho=0$ and $\rho=0.125$. Note how the high-temperature behavior is the same for both ferroelectric and relaxor systems. However, when the transition temperature is approached, the averaged cluster size tends to one for the ferroelectric (monodomain state) and grows slightly for the relaxor (glassy multidomain state).
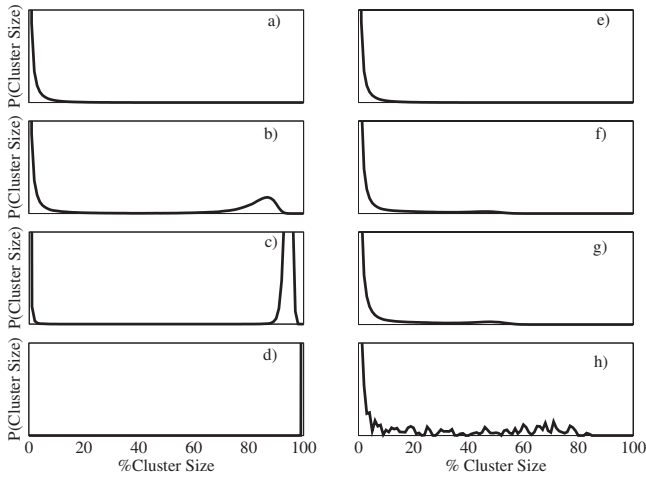
FIG. 9. Histogram of cluster sizes. The histogram is calculated by considering the number of times a cluster with a given size is formed in a Monte Carlo run at a given temperature. Temperatures considered are $T/T_c=7$ (a) ferroelectric (e) relaxor, $T/T_c=1.1$ (b) ferroelectric (f) relaxor, $T/T_c=1$ (c) ferroelectric (g) relaxor, and $T/T_c=0.25$ (d) ferroelectric (h) relaxor. Note how domains with appreciable sizes are formed for the relaxor only at the glassy phase but not at high temperature.

lyzed not just the averaged size but the complete histogram of cluster sizes (see Fig. 9). Temperatures considered are: high temperature $T/T_c=7$, close to the critical temperature $T/T_c=1.1$ at the critical temperature $T/T_c=1$ and below the critical temperature $T/T_c=0.25$. Formation of nanodomains with appreciable sizes are only found when the system is already at a temperature smaller than T_m.

These results indicate that no special high-temperature formation of nanoclusters is found for the relaxor when compared to the ferroelectric. Then, what are the microscopic differences between the ferroelectric and the relaxor? Why optic measurements,[11] diffusive scattering,[9] and high-resolution piezoresponse force microscope experiments[31] find nanodomains formation only for the relaxor?

To answer this question, it is important to take into account that no stability criterion or lifetime duration is considered on the numbering of clusters so every cluster formed is taken into account on our simulations. Next, we analyze not just the cluster size but the lifetime of the cluster. To do so, we calculate the percentage of slow dipoles (dipoles that flip less than 25% in a Monte Carlo run) versus temperature. In this case, the high-temperature behavior of the relaxor is clearly different from the ferroelectric and close to the temperature previously proposed as the Burns temperature, $T_d \sim 2T_c \gg T_m$ the number of slow dipoles increases dramatically (see Fig. 10). On the other hand, the ferroelectric dipoles are frozen just at $T=T_c$ because of the phase transition. So we may say that high-temperature clusters are the same for both, relaxor and ferroelectric models, but slow dipoles (detectable from the experimental point of view) are only found in the relaxor at $T < T_d$. How these frozen dipoles form nanoclusters with a net polarization different from zero at the glassy phase?

Snapshots of the relaxor at different temperatures $T/T_c=2,1.5,1.3,1.1,1,0.5$ are shown in Fig. 11. Itinerant charges
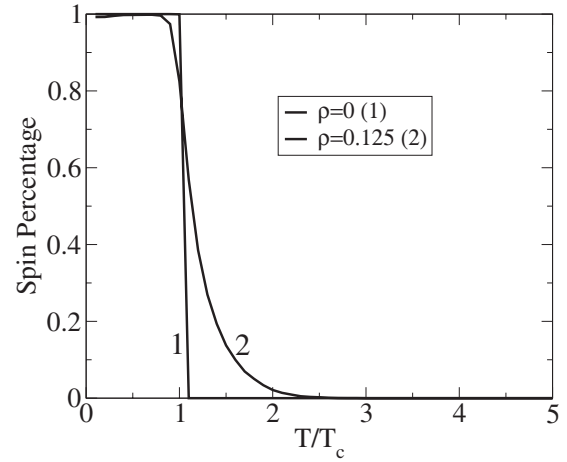

FIG. 10. Percentage of slow flipping-rate dipoles (see text) versus normalized temperature for $\rho=0.125$ and $\rho=0$. For the relaxor, slow dipoles are found well above the transition temperature.

are plotted together with slow dipoles. At the Burns temperature, some dipoles get trapped by the charges and first slow dipoles show up. As the system gets cooler, the number of these slow dipoles increases. The dipoles trapped by the charges form stable boundaries which will be the precursors of the ferroelectric microdomains found at the glassy phase at $T < T_m$. When the temperature approaches the critical temperature $T=T_c$, domains grow from the border toward the inside of the cluster. These clusters are stable, i.e., they are formed by dipoles with a low flipping rate. Each nanodomain is completed at a different temperature but at low enough temperature, all clusters are formed and the typical glassy state with charges trapped at the boundaries[32] shows up (see Fig. 11). The model shows how stable nanodomains (measured at $T < T_d$) are really the stable boundaries (and the precursors) of the domains found at the glassy state. It is impossible to find these stable boundaries in a regular ferro-
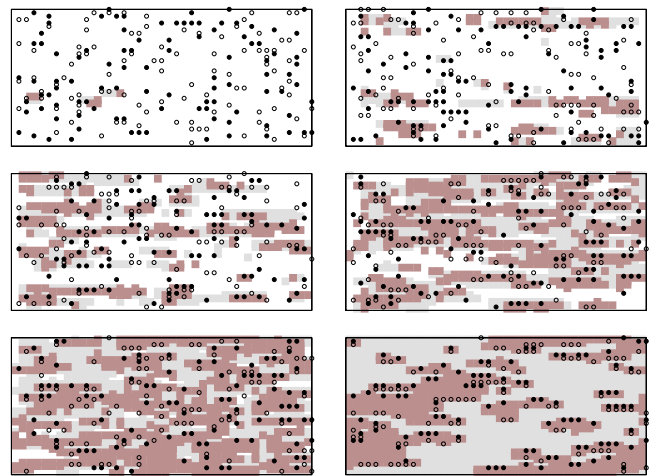

FIG. 11. (Color online) Snapshots of a relaxor ($\rho=0.125$) at different temperatures (a) $T/T_c=2$, (b) $T/T_c=1.5$, (c) $T/T_c=1.3$, (d) $T/T_c=1.1$, (e) $T/T_c=1$, and (f) $T/T_c=0.5$. Positive and negative charges (white and black circles) are represented together with up and down slow dipoles (dark and light gray squares).
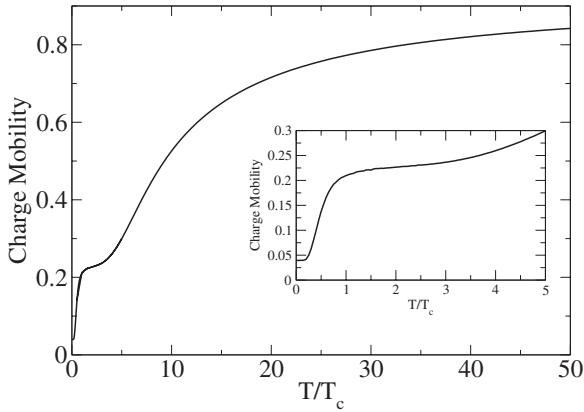
FIG. 12. Charge mobility (see text) vs normalized temperature for a relaxor system with $\rho=0.25$. Inset: detail at low temperatures.

electric material because there are no itinerant charges to trap the dipoles. From the point of view of dielectric dispersion with frequency, these slow dipoles contribute to the susceptibility only when the frequency of the electric field applied is low enough. If the frequency increases, slow dipoles are unable to follow field variations. Again it is impossible to find this effect in a ferroelectric, where no dipoles get trapped by the charges and no slow dipoles exist.

V. ITINERANT CHARGES MOVEMENT

The meaning of the Burns temperature may be also analyzed from the point of view of itinerant charges. Next we will study charge mobility versus temperature. Charge mobility is defined as the averaged number of accepted flips between sites divided by the total number of flip attempts. Results are shown in Fig. 12 for $\rho=0.25$. By cooling, mobility decreases smoothly until approximately $T=T_d$, then it remains almost constant. However, when the ferroelectric dipole-dipole interaction takes place at $T=T_c$, charge mobility decreases abruptly due to the multidomain formation at the glassy phase, reaching a maximum slope at $T=T_m$. To
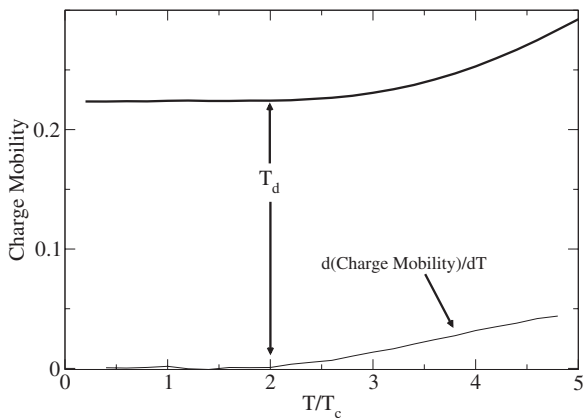

FIG. 13. Charge mobility (thick line) vs normalized temperature for a relaxor system with $\rho=0.25$ and no ferroelectric interaction $J=0$. Thin line represents the derivative of charge mobility with temperature. Note how mobility reaches a minimum at $T=T_d$.
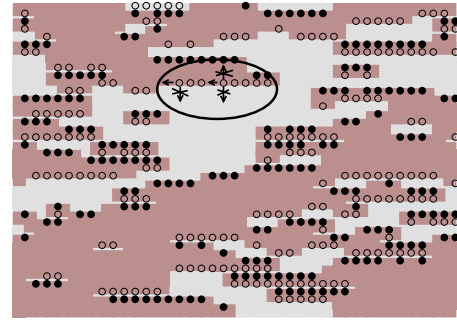

FIG. 14. (Color online) Snapshot of a multidomain relaxor configuration. Up and down configurations are shown by dark and light gray, respectively, while white and black circles represent positive and negative itinerant charges. Charges may move only along domain's border (see circle). Charges get stacked at the boundaries when slow dipoles border lines are formed.

clearly detect how the Burns temperature affects to charge mobility, we may set to zero the ferroelectric interaction in our simulations ($J=0$). Charges dipole J_q is now the only remaining interaction in the system. Results are shown in Fig. 13 together with the derivative of mobility with temperature. Now, the Burns temperature gets clearly defined as the temperature where mobility reaches its minimum, keeping constant by cooling. At $T=T_d$, when boundaries start to be formed, charges get trapped between different oriented dipoles. They may move along the borders but not crossing the boundaries in the direction of the dipoles (see Fig. 14). That is the reason why, when a monodomain is formed in a relaxor by an electric field, the stability of such a monodomain depends on whether this field is applied at a temperature T_E above or below the Burns temperature T_d.[19] If $T_E < T_d$, charges get trapped at boundaries of the ferroelectric monodomain and the monodomain turns stable by cooling. However, if $T_E > T_d$ itinerant charges may move across the main boundary forming new borders and a multidomain with net polarization equal to zero. Finally, we have also studied the charges drift velocity in the paraelectric region by study-
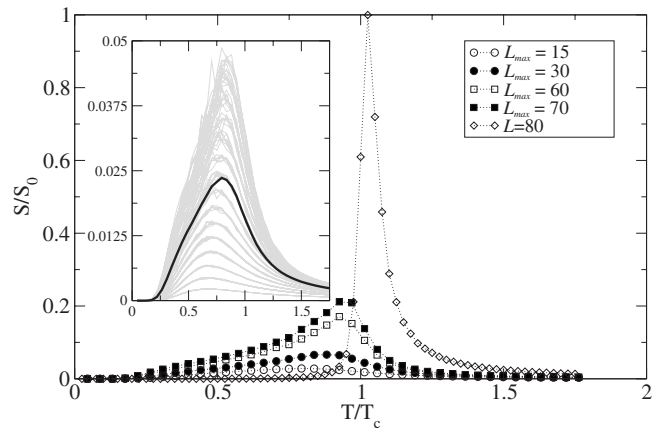

FIG. 15. Normalized susceptibility vs normalized temperature for a system made of domains with random lateral sizes ranging from $L=2$ to $L=L_{max}$. Inset shows the behavior of the susceptibility for $L_{max}=15$ in detail (thick line) together with the susceptibility curves of all domains averaged (light gray)

ing charges mobility when an external electric field is applied. Conductivity has been measured in the linear dependence region and an increase by increasing the temperature has been found. This behavior is not expected in metallic conductors but it is typical of insulating relaxor materials.[19]

VI. NANODOMAINS FORMATION AND THE ORIGIN OF THE MAXIMUM TEMPERATURE

In this section, we analyze the existence of a maximum temperature T_m that depends on charge-carrier density and the origin of the smearing of the transition in a relaxor. When the number of itinerant charge carriers is increased, the number dipoles belonging to a border line between domains grows and the average size of the domains gets smaller. We may simulate a multidomain system where size of the domains changes randomly between 2×2 and a fixed maximum size. Total susceptibility is obtained by averaging the susceptibilities coming from all the domains in the system which may be calculated separately on our simulations. Results for different values of the maximum domain size are shown in Fig. 15 compared to the monodomain ($L=80$) ferroelectric case. Clearly, as the size of the domains decreases, the temperature where susceptibility reaches its maximum tends to lower values (see inset). This is due to the lost of energy caused by the frustration of the dipoles at the boundaries of the domains. A strong dispersion in domain sizes produces a strong dispersion in the susceptibility curves and a smeared average response of the system. The maximum temperature T_m is the averaged value coming from the temperatures where each domain is formed.

VII. CONCLUSIONS

Using Monte Carlo calculations, we have analyzed the behavior of a microscopic relaxor model where no random interactions or fields are considered. The interaction between mobile charges and the dipoles of a highly polarizable medium is responsible for the appearance of relaxor properties. The model shows a temperature T_d below which the flipping rate of some dipoles, neighbors to the charges, decreases dramatically. These dipoles form stable boundaries from which ferroelectric clusters grow when approaching to the glassy phase. These frozen dipoles are also responsible for the frequency dispersion of the dielectric constant, smearing of the transition, and trapping of itinerant charges. T_d may be then associated to the Burns temperature.

ACKNOWLEDGMENTS

*manuel.marques@uam.es

[1] S.-E. Park and T. R. Shrout, J. Appl. Phys. **82**, 1804 (1997).

[2] G. A. Smolenskii, V. A. Isupov, A. I. Agranovskaya, and S. N. Popov, Sov. Phys. Solid State **2**, 2584 (1961).

[3] F. Chu, N. Stetter, and A. K. Tagantsev, J. Appl. Phys. **74**, 5129 (1993).

[4] X. Dai, Z. Xu, and D. Viehland, Philos. Mag. B **70**, 33 (1994).

[5] A. Krumins, T. Shiosaki, and S. Koizumi, Jpn. J. Appl. Phys., Part 1 **33**, 4940 (1994).

[6] P. H. Sciau, G. Calvarin, and J. Ravez, Solid State Commun. **113**, 77 (1999).

[7] A. Simon, J. Ravez, and M. Maglione, J. Phys.: Condens. Matter **16**, 963 (2004).

[8] N. Yasuda, H. Ohwa, and S. Asano Jpn. J. Appl. Phys., Part 1 **35**, 5099 (1996).

[9] L. E. Cross, Ferroelectrics **76**, 241 (1987).

[10] See, for instance, A. A. Bokov and Z.-G. Ye, J. Mater. Sci. **41**, 31, (2006); W. Kleemann, *ibid.* **41**, 129 (2006), and references therein.

[11] G. Burns and F. H. Dacol, Solid State Commun. **48**, 853 (1983); Phase Transitions **5**, 261 (1985).

[12] G. A. Smolenskii, J. Phys. Soc. Jpn. **28**, Suppl., 26 (1970).

[13] V. A. Isupov, Ferroelectrics **289**, 131 (2003).

[14] V. Westphal, W. Kleemann, and M. D. Glinchuk, Phys. Rev. Lett. **68**, 847 (1992).

[15] R. Fisch, Phys. Rev. B **67**, 094110 (2003).

[16] R. Pirc and R. Blinc, Phys. Rev. B **60**, 13470 (1999).

[17] H. Qian and L. Bursill, Int. J. Mod. Phys. B **10**, 2007 (1996);
10, 2027 (1996).

[18] M. I. Marqués and C. Aragó, Europhys. Lett. **71**, 124 (2005).

[19] T. Granzow, Th. Woike, M. Wöhlecke, M. Imlau, and W. Kleemann, Phys. Rev. Lett. **89**, 127601 (2002).

[20] E. Buixaderas, M. Savinov, M. Kempa, S. Veljko, S. Kamba, J. Petzelt, R. Pankrath, and S. Kapphan, J. Phys.: Condens. Matter **17**, 653 (2005).

[21] W. Kleemann, J. Dec, P. Lehnen, R. Blinc, B. Zalar, and P. Pankrath, Europhys. Lett. **57**, 14 (2002).

[22] W. Zhong, D. Vanderbilt, and K. M. Rabe, Phys. Rev. B **52**, 6301 (1995); M. I. Marqués, *ibid.* **71**, 174116 (2005).

[23] B. G. Potter, V. Tikare, and B. A. Tuttle, J. Appl. Phys. **87**, 4415 (2000); P. J. Schorn, U. Böttger, and R. Waser, Appl. Phys. Lett. **87**, 242902 (2005).

[24] J. Junquera and P. Ghosez, Nature (London) **422**, 506 (2003); M. I. Marqués and J. A. Gonzalo Nanotechnology **12**, 143 (2001).

[25] L. Onsager, Phys. Rev. **65**, 117 (1944).

[26] H. Gui, B. Gu, and X. Zhang, Phys. Rev. B **52**, 3135 (1995).

[27] A. M. Glass, J. Appl. Phys. **40**, 4699 (1969).

[28] A. Belous, O. Výunov, D. Mishchuk, S. Kamba, and D. Nuzhnyy, J. Appl. Phys. **102**, 014111 (2007).

[29] See, for instance, I. Rivera, A. Kumar, N. Ortega, R. S. Katiyar, and S. Lushnikov, Solid State Commun. **149**, 172 (2009).

[30] D. Viehland, S. J. Jang, and L. E. Cross, J. Appl. Phys. **68**, 2916 (1990).

[31] P. Lehnen, W. Kleemann, Th. Woike, and R. Pankrath, Phys. Rev. B **64**, 224109 (2001).

[32] A. G. Chynoweth, Phys. Rev. **117**, 1235 (1960).